SAE International

2012-01-0742
Published 04/16/2012

doi:10.4271/2012-01-0742
saealtpow.saejournals.org

Driving Pattern Recognition for Adaptive Hybrid Vehicle Control

Lei Feng, Wenjia Liu and Bo Chen
Michigan Technological Univ

ABSTRACT

The vehicle driving cycles affect the performance of a hybrid vehicle control strategy, as a result, the overall performance of the vehicle, such as fuel consumption and emission. By identifying the driving cycles of a vehicle, the control system is able to dynamically change the control strategy (or parameters) to the best one to adapt to the changes of vehicle driving patterns. This paper studies the supervised driving cycle recognition using pattern recognition approach. With pattern recognition method, a driving cycle is represented by feature vectors that are formed by a set of parameters to which the driving cycle is sensitive.

The on-line driving pattern recognition is achieved by calculating the feature vectors and classifying these feature vectors to one of the driving patterns in the reference database. To establish reference driving cycle database, the representative feature vectors for four federal driving cycles are generated using feature extraction method. The quality of representative feature vectors with different feature extraction methods is evaluated by examining the separation of feature vectors in the feature space and the success rate of the pattern recognition. The performance of the presented adaptive control strategy based on driving pattern recognition is evaluated using a powertrain/propulsion simulation and analysis software - Autonomie.

CITATION: Feng, L., Liu, W. and Chen, B., "Driving Pattern Recognition for Adaptive Hybrid Vehicle Control," *SAE Int. J. Alt. Power.* 1(1):2012, doi:10.4271/2012-01-0742.

1. INTRODUCTION

A hybrid electric vehicle (HEV) has better fuel economy and less emission than a conventional internal combustion engine vehicle due to the existence of electric powertrain. The introduction of additional powertrain components, however, makes the HEV control more challenging and the performance of HEVs is more sensitive to their control strategies. To achieve maximum fuel economy and minimum emissions, researchers in the automotive community have made significant effort to investigate the major factors impacting fuel efficiency and develop optimal power management strategies for hybrid vehicles [1,2,3,4,5]. Research results showed that, in addition to vehicle and fuel characteristics, driving patterns have a strong impact on the fuel consumption and exhaust emissions [6, 7]. To optimize vehicle performance, multi-mode driving control method has been proposed for the adaptive vehicle control [8, 9]. The multi-mode driving control is defined as the control strategy which is able to switch a current control algorithm to the one that is optimized to the recognized driving pattern [8]. The ability to dynamically select control algorithms based on identified driving patterns leads to adaptive vehicle control, improved energy efficiency, and reduced green gas emissions.

A driving pattern is typically defined as the driving cycle of a vehicle in a particular environment [10]. To recognize driving patterns, it is necessary to identify a list of characteristic parameters which can be used to describe driving patterns. Although there is no consensus among researchers about what parameters can be used for driving pattern recognition, several studies have attempted to find such a list of parameters. Ericsson [6] investigated the impact of 62 driving pattern parameters on fuel economy and emissions using a large amount of testing driving cycles. The study showed that nine driving pattern parameters (four associated with power demand and acceleration, three with gear changing behavior, and two with speed level) had an important effect on fuel consumption and emissions. Lin *et al.* [9] selected power demand related parameters and stop time for hybrid electric truck driving pattern recognition. In addition to vehicle parameters, Jeon *et al.* [8] incorporated road grade parameters in the driving pattern recognition. For pattern classification method, neural network [8], support vector machine (SVM) [11], and learning vector quantization

network [12] were applied for the driving pattern classification. However, most existing driving pattern recognition methods are based on binary classification, which may cause losing of information.

The importance of driving patterns to the fuel economy and emission justifies a systematic study of driving pattern recognition. In this paper, supervised pattern recognition approach is studied for the classification of a real-world driving cycle to a similar driving cycle in the representative driving cycle group. Four federal driving cycles, Urban Dynamometer Driving Schedule (UDDS), Highway Fuel Economy Driving Schedule (HWFET), a high acceleration aggressive driving schedule (US06), and an air conditioning driving schedule (SC03), are selected as representative driving cycles. These driving cycles represent different street types, driver behavior, and weather condition. With pattern recognition method, driving cycles and environmental information for various driving patterns are represented by corresponding features vectors. The classification is based on the distance of a test feature vector (test driving cycle) to the representative feature vectors (representative driving patterns). The test driving pattern is classified to one of representative driving pattern with which the test driving pattern has the smallest distance. The identified driving pattern information is then used to implement adaptive control strategies. The performance of adaptive control is evaluated in a powertrain/propulsion simulation and analysis software - Autonomie.

The rest of the paper is structured as follows. Section 2 introduces driving cycle classification based on the pattern recognition method. Section 3 presents the classification of real-world driving cycles using representative feature vectors of four federal driving cycles. Section 4 studies the impact of dissimilarity measures and feature extraction methods on the performance of driving cycle pattern recognition. Section 5 discusses adaptive vehicle control based on driving cycle pattern recognition. Section 6 concludes the presented work.

2. PATTERN-RECOGNITION-BASED DRIVING CYCLE RECOGNITION

2.1. CONCEPT OF PATTERN RECOGNITION

Pattern recognition is a scientific discipline whose goal is to classify objects into a number of meaningful categories or classes [13]. In pattern recognition, the patterns to be classified are usually the groups of measurements, defining points in an appropriate multidimensional space [13]. The measurements used for the classification are described by features. If p features are used f_i, i=1, 2… p, these p features can form a feature vector $F = (f_1, f_2,\ldots, f_p)^T$, where T denotes transposition. A feature vector is a point in P dimensional space R^P. The process of supervised pattern recognition consists of feature extraction and classification two steps. In the feature extraction stage, a number of feature members are selected from the measurement data of the pattern. These feature members are used to form feature vectors to represent the pattern. In the pattern classification stage, the dissimilarity of the test pattern with the representative patterns is evaluated. The dissimilarity of two patterns is defined as a function of the distance between the corresponding feature vectors of the patterns. Usually, the shorter distance means higher similarity and the longer distance means lower similarity. As such, the test pattern is classified to one of representative pattern with which the test pattern has the smallest distance. Different types of distance deifications can be used in pattern recognition. The Euclidian distance is one of the most commonly used distances. Let $X = (x_1, x_2,\ldots, x_n)^T$ and $Y = (y_1, y_2, y_2,\ldots,y_n)^T$ denote two feature vectors. The Euclidian distance between these two feature vectors is defined below:

$$d_{XY} = \sqrt{\left(\sum_{i=1}^{n}\left(x_i - y_i\right)^2\right)} \qquad (1)$$

2.2. FEATURE SELECTION FOR DRIVING CYCLE PATTERN RECOGNITION

Feature selection is application dependent. The rule of thumb for feature extraction is that the selected features can replicate most information of the original measurement data and separate feature vectors for different patterns in the feature space. To classify driving cycles, thirty-nine characteristic parameters were initially chosen based on Jeon and Ericsson's work [6, 8]. The high dimension of feature vectors, however, impedes practical application of driving cycle pattern recognition in real-time. To reduce the dimension of feature vectors, numerous simulation tests were performed to find a reduced set of feature members and the weighting factor for each feature member. The selection of the feature members and their weighting factors are based on if the representative feature vectors of individual driving cycles are clearly separated in the feature space. The simulation work finally identified fifteen feature members and corresponding weighting factors, listed in Table 1, to form feature vectors for driving cycles as shown below:

$$f = (k_1 \times a_1,\ k_2 \times a_2,\ \cdots\cdots,\ k_i \times a_i,\ \cdots\cdots,\ k_{15} \times a_{15})^T, \qquad i \in [1, 15] \qquad (2)$$

Where a_i is a feature member and k_i is a weighting factor

Table 1. Driving cycle feature members and corresponding weighting factors.

Index Number (i)	Feature Parameters (a)	Weighting Factor (k)
1	Average Cycle Speed (m/s)	10
2	Positive Average Acceleration (a>0.1m/s^2)	1
3	Low Speed Time (15-30 Km/h)/Total Time (%)	10
4	Mid High Speed Time (70-90 Km/h)/Total Time (%)	100
5	High Speed Time (>90 Km/h)/Total Time (%)	10
6	Extreme Deceleration Time (a<-2.5 m/s^2)/Total Time (%)	1000
7	High Deceleration Time (a<-2 & a>-2.5 m/s^2)/Total Time (%)	1
8	Maximum Cycle Acceleration (m/s^2)	100
9	Maximum Cycle Speed (Km/h)	6
10	Standard Deviation of Cycle Speed (Km/h)	1
11	Mid Deceleration Time (a<-1 & a>-1.5 m/s^2)/Total Time (%)	1000
12	Mid High Deceleration Time (a>-2 & a<-1.5 m/s^2)/Total Time (%)	1000
13	Mid Acceleration Time (a>1.5 & a<2 m/s^2)/Total Time (%)	1
14	High Acceleration Time (a>2 & a<2.5 m/s^2)/Total Time (%)	1000
15	Extreme Acceleration Time (a>2.5 m/s^2)/Total Time (%)	1000

2.3. REPRESENTATIVE FEATURE VECTORS FOR SELECTED DRIVING CYCLES

As discussed previously, a driving pattern is determined by multiple factors, including road type, driver behavior, and weather and traffic conditions. To form a good representative driving cycles base which are able to reflect aforementioned features, four federal driving cycles, UDDS, HWFET, US06, SC03, are selected as representative driving cycles. UDDS and HWFET are two driving cycles representing two road types. US06 represents the driver's behavior of aggressive driving. SC03 is chosen to represent the influence of humid weather. The profiles of these four driving cycles are shown in Figure 1, Figure 2, Figure 3, Figure 4. HWFET is a typical highway driving cycle featuring high speed and short stop time, while UDDS has the features of low average speed and long stop time. US06 has the highest average speed and presents extreme acceleration (a>2.5 m/s^2). SC03 is similar to UDDS but its acceleration is milder than that of UDDS due to the usage of air conditioner.

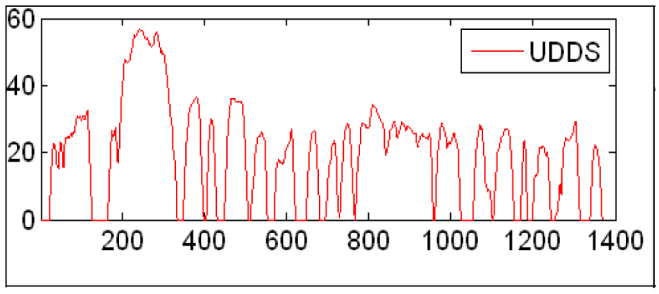

Figure 1. The driving cycle of UDDS.

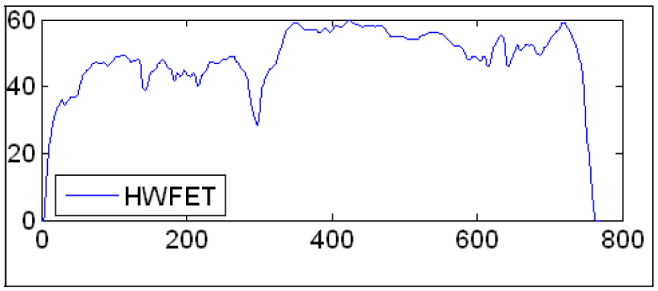

Figure 2. The driving cycle of HWFET.

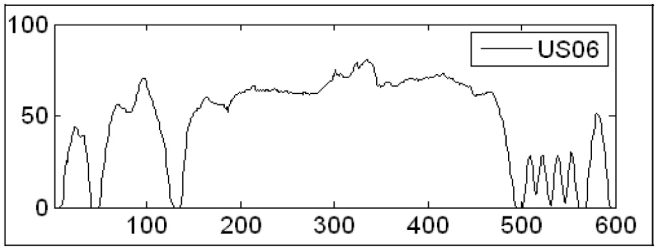

Figure 3. The driving cycle of US06.

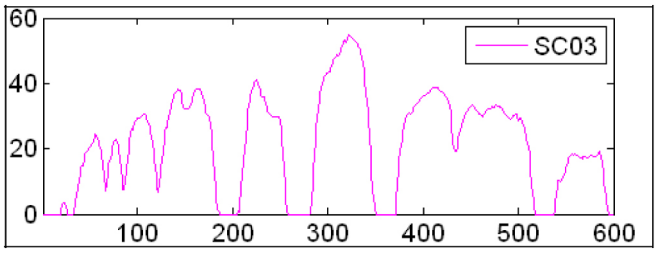

Figure 4. The driving cycle of SC03.

A feature vector of a driving cycle is calculated based on partial data points of a driving cycle for the quick recognition of driving cycle patterns, which is especially valuable in real-time applications. The number of data points is defined by the size of a sample window as shown in Figure 5. In this paper, the window size is set to 450 sample points. To speed up the recognition of driving cycle patterns, the technique of sequential processing of measurement is applied. As such, the next feature vector is calculated by advancing the sample window by 50 sample points. During real-time driving cycle pattern recognition, vehicle controllers collect a number of data points defined by the size of the sample window and calculate a feature vector for the current sample window using parameters defined in Table 1. The real driving cycle is then classified to one of four representative driving cycles using classification algorithms and calculated feature vector. Once the driving cycle is recognized, the control algorithm/ parameters are switch to the one that is optimal to recognized driving pattern. The time between one control decision points to the next control decision point is 50 seconds in this study if the sample rate is 1 Hz.

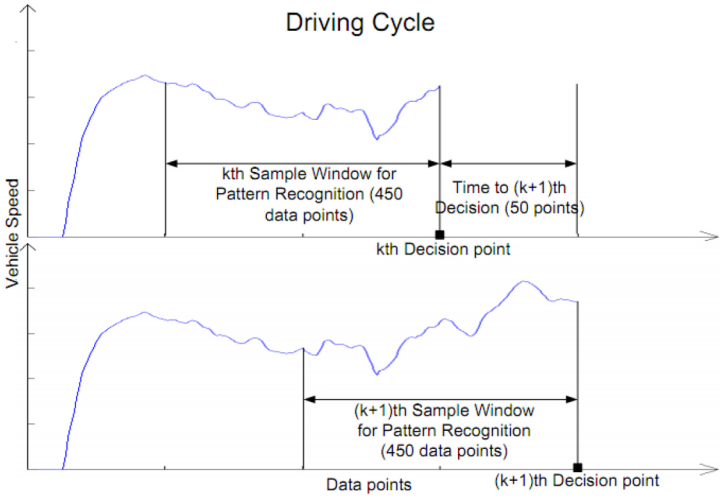

Figure 5. The definition of sample window and sequential processing of measurements.

To generate the representative feature vectors for the UDDS, HWFET, US06, and SC03, the velocity data for these driving cycles were downloaded from the U.S. Environmental Protection Agency website[14]. By comparing the speed profiles, the beginning part of the UDDS and US06 are similar to each other. To correctly distinguish UDDS and US06 driving cycles, the most representative data segments were used to generate feature vectors for the corresponding driving cycles. For the UDDS, velocity data starting from 347th second to the end of the driving cycle were used since this segment contains frequent stops, which is the major feature of the UDDS. For the US06 cycle, velocity data starting from 134th second to the end of the driving cycle were used. This segment differs from UDDS and represents the aggressive feature of driving (large accelerations). Since these representative segments have different lengths, a common data length of 2000 data points was specified to ensure the same number of representative feature vectors for each driving cycle. The representative segment for each driving cycle was repeated to form a data set with a length of 2000. In each data set, the first 450 data points were used to form the first sample window and find the first feature vector using equation (2). The second feature vector was calculated by advancing the sample window by 50 data points. From equation (2) we can see that the dimension of feature vectors is 15. To display high dimensional driving cycle feature vectors, the Principal Component Analysis (PCA) algorithm was applied to the generated representative feature vectors. The first and second principal components were then used to plot representative feature vectors in 2-dimensional space. Figure 6 shows the distribution of representative feature vectors for the selected four driving cycles.

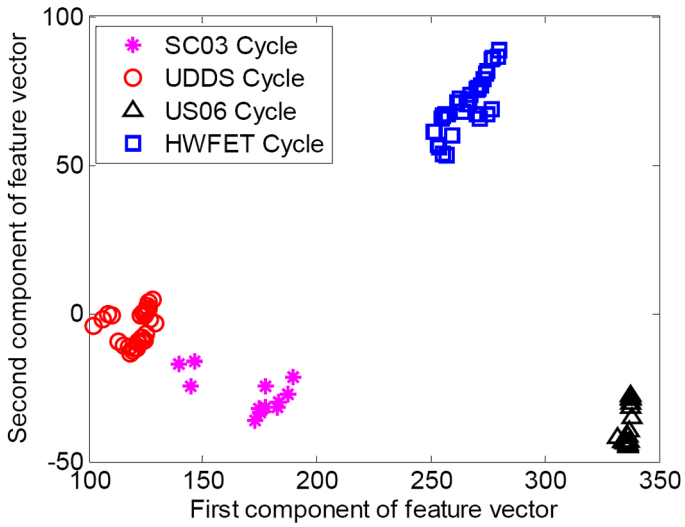

Figure 6. The distribution of the feature vectors of selected four driving cycles.

3. CLASSIFY REAL WORLD DRIVING CYCLES USING REPRESENTATIVE FEATURE VECTORS

To validate the effectiveness of representative feature vectors for real-world driving cycle pattern recognition, two real-world driving cycles were adopted for the performance test. The two real-world driving cycles were collected by a mild-hybrid Chevy Malibu driven in the urban and suburban area near the downtown Hancock. The routes of real-world city cycle (RW-CC) and real-world highway cycle (RW-HC) are shown in Figure 7 and Figure 8. The speed profiles for these two driving cycles are shown in Figure 9 and Figure 10. To classify real-world driving cycles to one of the selected four driving cycles, the feature vectors for the RW-CC and RW-HC were generated using the feature extraction method

described in Section 2. The classification is to identify to which pattern the test pattern belongs. The *k*-Nearest Neighbor (*k*NN) algorithm was employed for the driving cycle classification. For a test feature vector x, the nearest neighbor rule is summarized as follows. (1) Calculate the distances of the test feature vector x to each of representative feature vectors shown in Figure 6. (2) Identify the k nearest neighbors of representative feature vectors to the vector x. The number of k is general not to be a multiple of the number of classes M. (2) Out of these k samples, identify the number of vectors, k_i, that belong to class ω_i, $i = 1, 2, \ldots\ldots, M$, $\Sigma_i k_i = k$. (3) Assign x to the class ω_i with the maximum number k_i of samples. In the real-world driving cycle test, the value of M is 4 and the number of k is chosen to be 13. The distances between the test feature vector and representative feature vectors was calculated by the Euclidean distance.

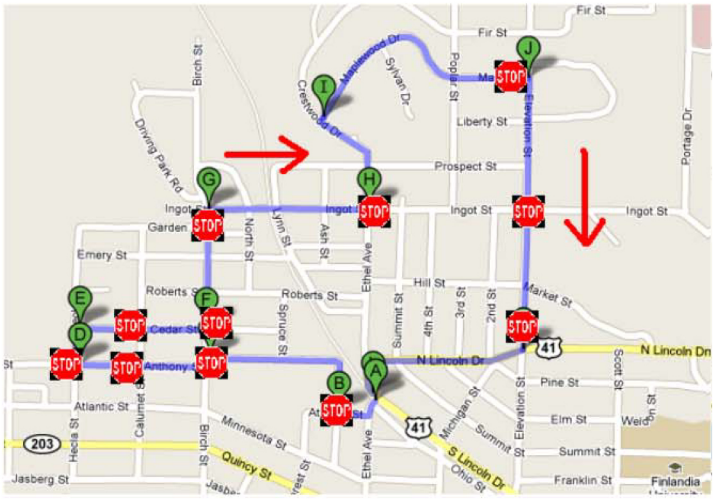

Figure 7. The route of city cycle.

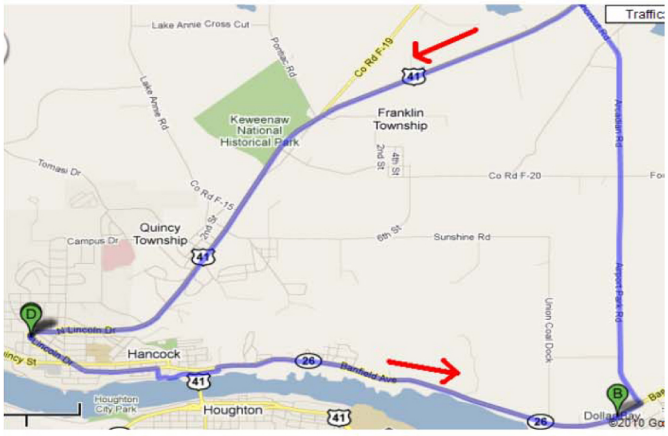

Figure 8. The route of highway cycle.

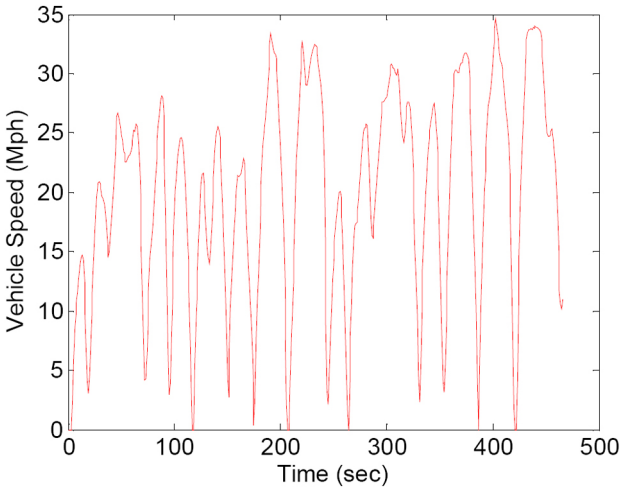

Figure 9. The speed profile of city cycle.

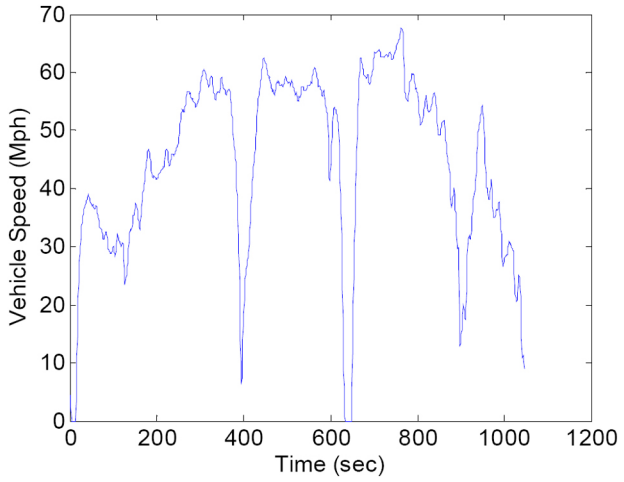

Figure 10. The speed profile of highway cycle.

The success rates of classifying the RW-CC to the UDDS category and the RW-HC to the HWFET are shown in Figure 11. In the classification test, the success rate of driving cycle pattern recognition was calculated with different size of the sample window. The tested sample window sizes include 50, 100, 150, 200, 250, 300, 350, 400, and 450. Figure 11 show that the larger size of the sample window has a higher pattern recognition success rate for both RW-CC and RW-HC. In addition, the success rates of the RW-CC are higher than RW-HC. This is due to the fact that the similarity of the RW-CC with the UDDS is higher than the similarity of the RW-HC with the HWFET.

4. PERFORMANCE STUDY

This section studies the impact of the dissimilarity measures and the feature extraction methods on the quality of representative feature vectors and the performance of the driving cycle pattern recognition.

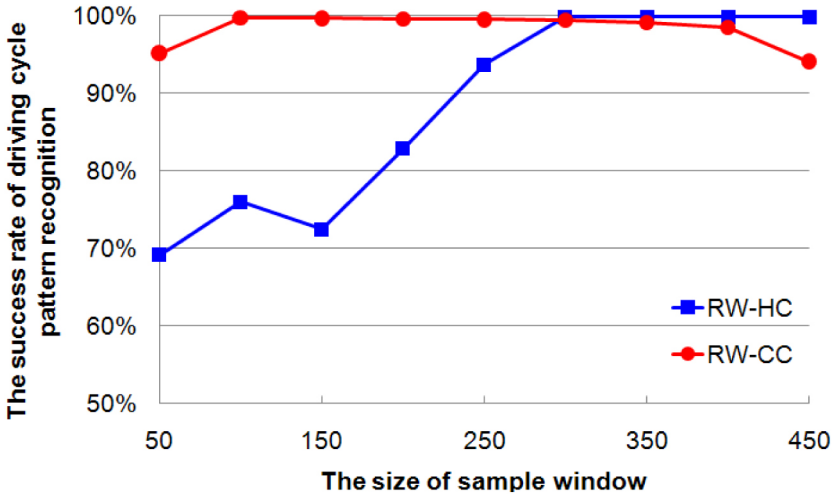

Figure 11. The success rate of real world driving cycle pattern recognition.

4.1. THE IMPACT OF DISSIMILARITY MEASURES ON PATTERN RECOGNITION SUCCESS RATE

To test the impact of the dissimilarity measure (distance between feature vectors) on the performance of the pattern recognition, a number of dissimilarity measures were tested for the driving cycle pattern recognition. The tested similarity measures include Euclidean distance, Chebyshev distance, Cosine distance, Correlation distance, and Mahalanobis distance. Let X and Y are two feature vectors with dimension *n*. The definitions of these dissimilarity measures are given below:

• Chebyshev distance:

$$d_{XY} = \max(|X_i - Y_i|), i \in n \tag{3}$$

• Cosine distance:

$$d_{XY} = 1 - \frac{XY^T}{\left(XX^T\right)^{1/2}\left(YY^T\right)^{1/2}} \tag{4}$$

• Correlation distance:

$$d_{XY} = 1 - \frac{\left(X-\overline{X}\right)\left(Y-\overline{Y}\right)^T}{\left(\left(X-\overline{X}\right)\left(X-\overline{X}\right)^T\right)^{1/2}\left(\left(Y-\overline{Y}\right)\left(Y-\overline{Y}\right)^T\right)^{1/2}} \tag{5}$$

Where $\overline{X} = \frac{1}{p}\sum_j X_j, \overline{Y} = \frac{1}{p}\sum_j Y_j$

• The Mahalanobis distance of a multivariate vector $X = (x_1, x_2, \ldots\ldots, x_n)^T$ from a group of values with mean $\mu = (\mu_1, \mu_2, \ldots\ldots, \mu_n)^T$ and covariance matrix S is defined as:

$$D = \sqrt{(X-\mu)^T S^{-1}(X-\mu)} \tag{6}$$

Figure 12 shows the success rate of RW-CC pattern recognition with various dissimilarity measures using *k*NN 13 classification method. From Figure 12 we can see that the Euclidean distance is the only dissimilarity measure that has good pattern recognition performance for the RW-CC pattern recognition. Other dissimilarity measures, including Cosine distance, Correlation distance, and Mahalanobis distance have very bad performance for the RW-CC pattern recognition. The average success rate of the Chebyshev distance is only about 60% and it fluctuates significantly. Figure 13 shows the success rate of RW-HC pattern recognition with aforementioned dissimilarity measures. The Mahalanobis distance shows the best performance of the RW-HC pattern recognition. The Euclidean distance and the Chebyshev distance also show the good performance when the sample window size is larger than 300 data points.

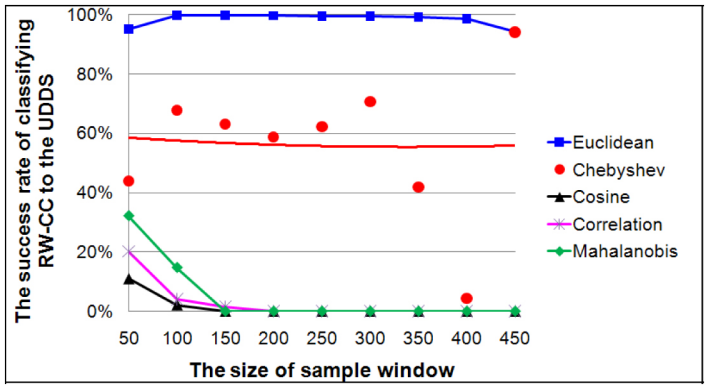

Figure 12. The success rate of real city cycle recognition using KNN-13 with various dissimilarity measures.

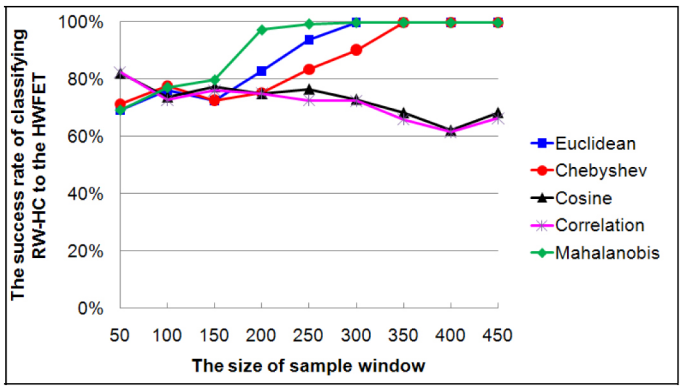

Figure 13. The success rate of real highway cycle recognition using KNN-13 with various dissimilarity measures.

4.2. THE IMPACT OF FEATURE EXTRACTION METHODS ON THE QUALITY OF REPRESENTATIVE FEATURE VECTORS

Various feature extraction methods have been proposed to extract features from time series sensor data, such as Single Value Decomposition [15], Discrete Fourier Transformation [16, 17], Discrete Wavelet Transformation [18], Adaptive Piecewise Constant Approximation [19], Discrete Cosine Transformation [15], Chebyshev Polynomials [20], Piecewise Aggregate Approximation [21], and Symbolic Aggregate Approximation [22]. In this section, the performance of the autoregressive (AR), DFT, and DWT feature extraction methods for the driving cycle pattern recognition is studied.

4.2.1. Feature Extraction using Auto-Regressive Model

For the normalized driving cycle data set X, it can be fitted to an AR model of order p as

$$x_k = \sum_{i=1}^{p} \alpha_i x_{k-i} + r_k \quad k = p+1,\ldots,n \tag{7}$$

Where α_i, $i = 1,2,\ldots, p$ is a coefficient of the AR model; r_k, $k = p + 1,\ldots, n$ is the residual between the driving cycle data and the AR model value. The vector $f(X) = (\alpha_1, \alpha_2,\ldots, \alpha_p)^T$ can be used as the feature vector of the normalized data X.

4.2.2. Feature Extraction using Discrete Fourier Transform

Discrete Fourier Transform is one of techniques for dimensionality reduction using spectral decomposition. In this study, the DFT coefficients of the four driving cycle data vary a lot within the frequency range 0-0.5Hz. The frequency range 0-0.5Hz was equally divided into 5 small ranges, each of which has 0.1Hz bandwidth. In each small range, the frequency with largest amplitude was selected as a feature member. The mean value of the DFT amplitudes in each small frequency range was also selected as a feature member. As such, the feature vector was formed by frequencies f_1 - f_5 and the mean amplitudes a_1 - a_5 as shown below

$$f(X) = (f_1,\ k\times a_1,\ f_2,\ k\times a_2,\ f_3,\ k\times a_3,\ f_4,\ k\times a_4,\ f_5,\ k\times a_5)^T \tag{8}$$

where k is the weighting factor of the amplitudes.

4.2.3. Feature Extraction using Discrete Wavelet Transform

Discrete wavelet transform decomposes a signal into layers of coefficients. These coefficients contain both frequency and time domain information. Given a time series x with the length of n, the discrete wavelet transform of x is calculated by passing the time-series data through a series of low pass and high pass filters. The outputs from the high pass filter are called detail coefficients while the outputs from the low-pass filter are called approximation coefficients. The approximation coefficients are further decomposed in the next iteration while the detail coefficients are kept as the current level wavelet coefficients. To form feature vectors from wavelet coefficients, feature extraction method proposed in [23] was employed, which consists of two steps: cluster determination and feature determination. The cluster determination process determines the boundary of each cluster in DWT coefficients matrix, while the feature determination step calculates each element of the feature vector using the Euclidean norms of coefficients in each cluster.

4.2.4. Success Rate of the Pattern Recognition using AR, DFT, and DWT Feature Extraction Methods

Autoregressive, discrete Fourier transformation, and discrete wavelet transformation feature extraction methods were applied to the UDDS, HWFET, US06, and SC03 driving cycle data. The generated representative feature vectors for these four driving cycles are shown in Figure 14, Figure 15, Figure 16. The features vectors generated using AR, DFT, and DWT methods are not well separated. With these representative feature vectors, the success rates of driving cycle pattern recognition were tested using kNN-9 classification method and Euclidean distance. The test results are shown in Figure 17, Figure 18, Figure 19. As we can see from these figures, the success rates, in generally, are lower than the pattern recognition success rate using representative feature vectors shown in Figure 6. Although the DFT feature extraction method has high success rates for the RW-CC

pattern recognition, the success rates for the RW-HC pattern recognition is extremely low.

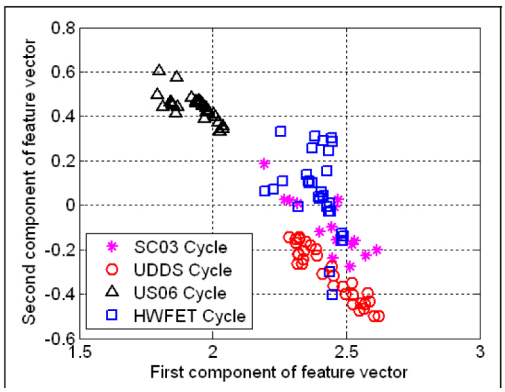

Figure 14. The distribution of AR-based feature vectors.

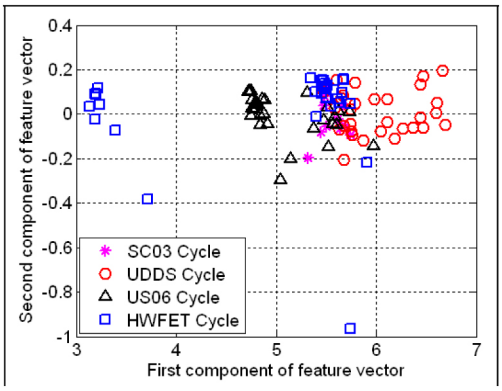

Figure 15. The distribution of DFT-based feature vectors.

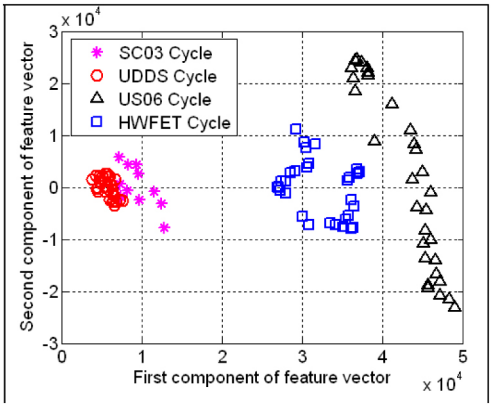

Figure 16. The distribution of DWT-based feature vectors.

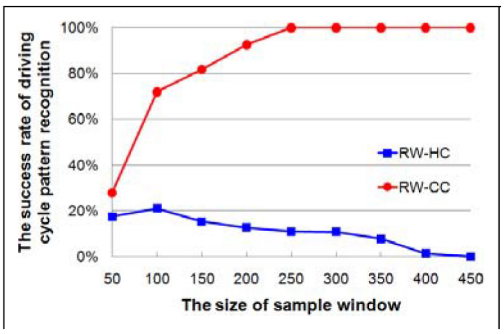

Figure 17. Success rate of pattern recognition using AR based feature extraction method.

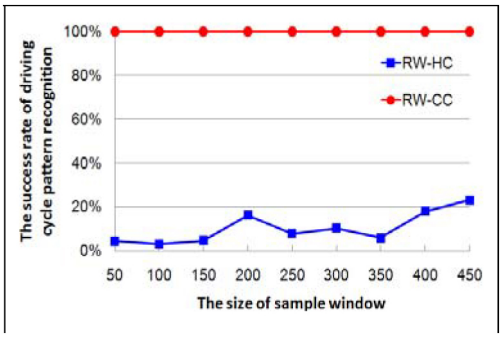

Figure 18. Success rate of pattern recognition using DFT based feature extraction method.

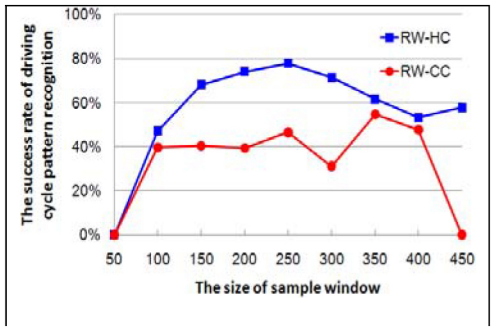

Figure 19. Success rate of pattern recognition using DWT based feature extraction method.

5. ADAPTIVE CONTROL BASED ON DRIVING CYCLE PATTERN RECOGNITION

The adaptive control is achieved through the real-time driving cycle pattern recognition and dynamic change the control parameters that are optimized to the recognized driving cycle. To implement this adaptive control strategy in a vehicle model, optimal control parameters for each representative driving cycle need to be identified. The simulation software and the vehicle model used to evaluate

Table 2. Default and optimized controller gains.

		Default Gains	Optimized Controller Gains			
			UDDS	US06	SC03	HIGHWAY
Controller Gains	Driver Controller Ki	0.5	0.2	0.1	0.5	0.4
	Driver Controller Kp	1000	500	500	500	500
	Motor 2 Ki	0.005	0.01	0.001	0.007	0.005
	Motor 2 Kp	0.5	0.8	0.6	0.9	0.7
Fuel Economy with default gains			72.38	43.28	69.83	63.30
Fuel Economy with optimized gains			73.56	44.03	71.67	63.35
Improved Percentage			1.63%	1.73%	2.63%	0.08%

the improvement of fuel economy for the proposed adaptive control are the powertrain/propulsion simulation and analysis software - Autonomie [24] and the Prius MY04 model.

5.1. OPTIMIZED CONTROLLER GAINS FOR INDIVIDUAL DRIVING CYCLES

The Prius MY04 model in Autonomie has three major modules: the driver controller module, the powertrain controller module, and the vehicle powertrain architecture module. The driver controller module determines how much power is needed from the vehicle powertrain according to the difference between the target vehicle speed and the actual vehicle speed. The powertrain controller module determines the torque demands of the engine, motor 1, and motor 2. The simulation results showed that the proportional and integral gains of the two controllers; one is the driver controller and the other one is the motor 2 controller, affect the fuel economy of the vehicle under different driving cycles. To reduce fuel consumption, these four controller parameters are selected to dynamically change during the fuel economy simulation for different input driving cycles. To find optimal controller gains for different driving cycles, 36 simulations are carried out for each representative driving cycle and 144 simulations in total are conducted for 4 federal driving cycles. When one optimal gain is being searched, the values of other 3 gains are fixed. The final optimized controller gains for four federal driving cycles are listed in Table 2.

5.2. THE IMPROVEMENT OF FUEL ECONOMY WITH DYNAMIC SELECTION OF CONTROLLER GAINS BASED ON DRIVING CYCLE PATTERN RECOGNITION

To evaluate the performance of the proposed adaptive control based on the driving cycle pattern recognition, the pattern recognition algorithm is integrated with the Prius MY04 vehicle model in Autonomie. The output value of the pattern recognition algorithm for SC03, UDDS, US06, HWFET, and unclassified driving cycle (when the data points is less than 300) is defined as 1, 2, 3, 4, and 0, respectively. During simulation, a combination of three real-world city cycle (RW-CC) plus one real-world highway cycle (RW-HC) is input into the simulation. The pattern recognition result for this combination is shown in Figure 20. As we can see from Figure 20, the pattern recognition result is 0 in the first 300 seconds (data sample rate is 1 Hz) because there is not enough data points for pattern recognition. After 300 seconds, the pattern recognition algorithm successfully classifies the input driving cycle to urban driving cycle. At 1398th second, three real-world city cycle ends and the real-world highway cycle starts. When the data points from the real-world highway cycle add to the pattern recognition data buffer, the buffer contains speed data both from real-world city cycle and real-world highway cycle. This causes the fail of pattern recognition from 1570th second to 1690th second. After 1690 seconds, most speed data in the pattern recognition data buffer are from the real-world highway cycle, as a result, the pattern recognition algorithm is able to successfully classify the current driving cycle to highway driving cycle. The output of the pattern recognition algorithm is then used to select new controller gains to which the recognized driving pattern has the highest fuel economy.

A comparison of fuel economy with default and optimized controller gains is conducted. The input driving cycles are a combination of real-world city cycle and real-world highway cycle and a combination of four federal driving cycles. The simulation result shows that the optimized controller gains have better fuel economy in both cases. The improvement of fuel economy for two different combinations of driving cycles is shown in Table 3.

6. CONCLUSIONS AND FUTURE WORK

Driving cycle recognition based on the pattern recognition methodology is presented in this paper. In this approach, a driving cycle is represented by feature vectors. These feature vectors are formed by a number of features and

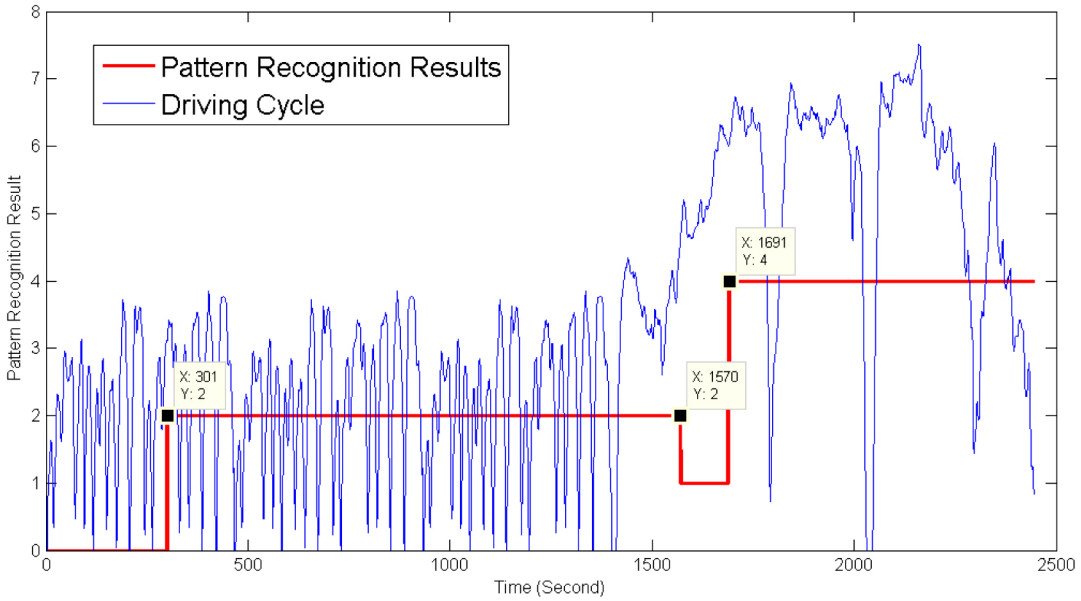

Figure 20. Pattern recognition result for real-world city cycle and real-world highway cycle.

Table 3. The improvement of fuel economy with adaptive controller based on driving cycle pattern recognition

Driving cycle	Fuel economy with default controller gains (Miles per gallon)	Fuel economy with optimized controller gains (Miles per gallon)	Fuel economy improvement in percentage
3 RW-CC + 1 RW-HC	61.87	62.51	1.03%
SC03+UDDS+HW+US06	59.09	60.05	1.60%

corresponding weighting factors. In order to classify a real-world driving cycle to one of the driving cycles in a reference database, four federal driving cycles: UDDS, HWFET, US06, and SC03 are used to form this reference driving cycle database. Fifteen feature parameters to which four federal driving cycles are sensitive and corresponding weighting factors are identified to form the representative feature vectors for the four driving cycles. The performance of the presented driving cycle pattern recognition method and the impact of the dissimilarity measures and the feature extraction methods on the success rate of the driving cycle pattern recognition and the quality of representative feature vectors are investigated using two real world driving cycles: real-world highway cycle and real-world city cycle. The evaluation result shows that the size of sample window, the type of dissimilarity measures, and the feature extraction method have a great impact on the performance of driving cycle pattern recognition. The presented pattern recognition algorithm is integrated with the Prius MY04 vehicle model in Autonomie. The effectiveness of the adaptive control is studied by comparing the fuel economy of adaptive control with the fuel economy of fixed control parameters when a combination of different driving cycles is inputted into the model. The simulation results show that the adaptive control can improve the fuel economy up to 2.63%. In the future study, driving patterns representing factors such as driver behavior, traffic condition, and the weather condition, will also be investigated to realize more comprehensive driving pattern recognition and thus greater fuel economy improvement. In addition, dynamic selection of control strategies for different driving patterns will also be studied.

REFERENCES

1. Moura, S. J., Fathy, H. K., Callaway, D. S., and Stein, J. L., "A Stochastic Optimal Control Approach for Power Management in Plug-In Hybrid Electric Vehicles," *IEEE Transactions on Control Systems Technology*, Vol. 19, pp. 545-555, May 2011.
2. Liu, J. and Peng, H., "Modeling and control of a power-split hybrid vehicle," *IEEE Transactions on Control Systems Technology*, Vol. 16, Nov. 2008.
3. Borhan, H. A., Vahidi, A., Phillips, A. M., Kuang, M. L., and Kolmanovsky, I. V., "Predictive energy management of a power-split hybrid electric vehicle," *2009 American Control Conference (ACC-09)*, 01 2009.
4. Serrao, L., Onori, S., and Rizzoni, G., "A Comparative Analysis of Energy Management Strategies for Hybrid Electric Vehicles," *Journal of Dynamic Systems Measurement and Control-Transactions of the Asme*, Vol. 133, May 2011.
5. Sciarretta, A. and Guzzella, L., "Control of hybrid electric vehicles," *IEEE Control Systems Magazine*, Vol. 27, pp. 60-70, Apr 2007.
6. Ericsson, E., "Independent Driving Pattern Factors and their Influence on Fuel-use and Exhaust Emission Factors," *Transportation Research Part D-Transport and Environment*, Vol. 6, pp. 325-345, Sep 2001.
7. Ericsson, E., "Variability in Urban Driving Patterns," *Transportation Research Part D-Transport and Environment*, Vol. 5, pp. 337-354, Sep 2000.
8. Jeon, S. I., Jo, S. T., Park, Y. I., and Lee, J. M., "Multi-mode Driving Control of a Parallel Hybrid Electric Vehicle Using Driving Pattern Recognition," *Journal of Dynamic Systems Measurement and Control-Transactions of the Asme*, Vol. 124, pp. 141-149, Mar 2002.

9. Lin, C. C., Jeon, S., Peng, H., and Lee, J. M., "Driving pattern recognition for control of hybrid electric trucks," *Vehicle System Dynamics*, Vol. 42, pp. 41-58, Jul-Aug 2004.
10. Bata, R., Yacoub, Y., Wang, W., Lyons, D. et al., "Heavy Duty Testing Cycles: Survey and Comparison," SAE Technical Paper 942263, 1994, doi: 10.4271/942263.
11. Zhang, L., Zhang, X., Tian, Y., and Zhang, X., "Intelligent Energy Management Based on the Driving Cycle Sensitivity Identification Using SVM," presented at the 2009 Second International Symposium on Computational Intelligence and Design, 2009.
12. Langari, R. and Won, J. S., "Intelligent energy management agent for a parallel hybrid vehicle - Part 1: System architecture and design of the driving situation identification process," *Ieee Transactions on Vehicular Technology*, Vol. 54, pp. 925-934, May 2005.
13. Theodoridis, S. and Koutroumbas, K., *Pattern Recognition* Academic Press, 2008.
14. U. S. E. P. Agency. (2010). *Testing and Measuring Emissions* Available: http://www.epa.gov/nvfel/testing/dynamometer.htm
15. Korn, F., Jagadish, H. V., and Faloutsos, C., "Efficiently supporting ad hoc queries in large datasets of time sequences," *Sigmod Record*, Vol. 26, pp. 289-300, June 1997.
16. Agrawal, R., Faloutsos, C., and Swami, A., "Efficient similarity search in sequence databases," in *Proc. of the 4th Conference on Foundations of Data Organization and Algorithms*, 1993.
17. Faloutsos, C., Ranganathan, M., and Manolopoulos, Y., "Fast subsequence matching in time-series databases," *Sigmod Record*, Vol. 23, pp. 419-429, 1994.
18. Kin-Pong, C. and Ada Wai-Chee, F., "Efficient time series matching by wavelets," in *Proceedings of IEEE Computer Society 15th International Conference on Data Engineering*, Sydney, NSW, Australia, 1999, pp. 126-133.
19. Keogh, E., Chakrabarti, K., Mehrotra, S., and Pazzani, M., "Locally adaptive dimensionality reduction for indexing large time series databases," *Sigmod Record*, Vol. 30, pp. 151-162, Jun 2001.
20. Cai, Y. and Ng, R., "Indexing spatio-temporal trajectories with Chebyshev polynomials," in *International Conference on Management of Data* Paris, France, 2004, pp. 599-610.
21. Keogh, E., Chakrabarti, K., Pazzani, M., and Mehrotra, S., "Dimensionality reduction for fast similarity search in large time series databases," *Knowledge and Information Systems*, Vol. 3, pp. 263-286, August 2001.
22. Lin, J., Keogh, E., Wei, L., and Lonardi, S., "Experiencing SAX: a novel symbolic representation of time series," *Data Mining and Knowledge Discovery*, Vol. 15, pp. 107-144, Oct 2007.
23. Pittner, S. and Kamarthi, S. V., "Feature extraction from wavelet coefficients for pattern recognition tasks," *IEEE Transactions on Pattern Analysis and Machine Intelligence*, Vol. 21, pp. 83-88, 1999.
24. *Autonomie - Vehicle Modeling and Development Environment*. Available: http://www.autonomie.net/

CONTACT INFORMATION

Bo Chen, PhD
Assistant Professor
Department of Mechanical Engineering - Engineering Mechanics
Department of Electrical and Computer Engineering
Michigan Technological University
bochen@mtu.edu
http://www.imes.mtu.edu

Lei Feng
MS Student
Department of Mechanical Engineering - Engineering Mechanics
Michigan Technological University
leifeng@mtu.edu

Wenjia Liu
PhD Student
Department of Electrical and Computer Engineering
Michigan Technological University
wenjial@mtu.edu

ACKNOWLEDGMENTS

This material is based upon work supported by the National Science Foundation under Grant No. CMMI-1049294 and EEC-1062886. Any opinions, findings, and conclusions or recommendations expressed in this material are those of the authors and do not necessarily reflect the views of the sponsoring institution.

DEFINITIONS/ABBREVIATIONS

HEV
hybrid electric vehicle
SVM
support vector machine
UDDS
urban dynamometer driving schedule
HWFET
highway fuel economy driving schedule
US06
a high acceleration aggressive driving schedule
SC03
an air conditioning driving schedule
PCA
the principal component analysis
RW-CC
real-world city cycle
RW-HC
real-world highway cycle
kNN
The *k*-Nearest Neighbor
AR
autoregressive
DFT
discrete Fourier transform
DWT
discrete wavelet transform